Sanger, F. (1981) *Science 214*, 1205–1210.
Scouloudi, H., & Baker, E. N. (1978) *J. Mol. Biol. 126*, 637–660.
Shulman, R. G., Wüthrich, K., Yamane, T., Patel, D. J., & Blumberg, W. E. (1970) *J. Mol. Biol. 53*, 143–157.
Smith, M. C., & McLendon, G. (1980) *J. Am. Chem. Soc. 102*, 5666–5670.
States, D. J., Haberkorn, R. A., & Ruben, D. J. (1982) *J. Magn. Reson. 48*, 286–292.
Steadman, J. H., Yates, A., & Huehns, E. R. (1970) *Br. J. Haematol. 18*, 435–446.
Takano, T. (1977) *J. Mol. Biol. 110*, 537–568.
Teale, F. W. J. (1959) *Biochim. Biophys. Acta 35*, 543.
Varadarajan, R. (1988) Ph.D. Thesis, Stanford University.
Varadarajan, R., Szabo, A., & Boxer, S. G. (1985) *Proc. Natl. Acad. Sci. U.S.A. 82*, 5681–5684.
Varadarajan, R., Zewert, T. E., Gray, H. B., & Boxer, S. G. (1989) *Science 243*, 69–72.
Warshel, A., & Russell, S. T. (1985) *Q. Rev. Biophys. 17*, 283–422.
Warwicker, J., & Watson, H. C. (1982) *J. Mol. Biol. 157*, 671–679.
Wolfenden, R., Anderson, L., Cullis, P. M., & Southgate, C. C. B. (1981) *Biochemistry 20*, 849–855.
Wright, K. A., & Boxer, S. G. (1981) *Biochemistry 20*, 7546–7556.
Wüthrich, K. (1986) *NMR of Proteins and Nucleic Acids*, p 17, Wiley, New York.

Amino Acid Sequences of Pyridoxal 5′-Phosphate Binding Sites and Fluorescence Resonance Energy Transfer in Chicken Liver Fatty Acid Synthase†

Soo-Ik Chang and Gordon G. Hammes*
Department of Chemistry, Cornell University, Ithaca, New York 14853-1301
Received November 29, 1988; Revised Manuscript Received January 13, 1989

ABSTRACT: The amino acid sequences associated with pyridoxal 5′-phosphate binding sites in chicken liver fatty acid synthase have been determined: a site whose modification causes selective inhibition of the enoyl reductase activity and a site (site I) that is not associated with enzymatic activity. The amino acid sequences of peptides obtained by trypsin hydrolysis of the pyridoxamine 5′-phosphate labeled enzyme were determined. For the site associated with enoyl reductase activity, the sequence similarities between chicken and goose are extensive and include the sequence Ser-X-X-Lys, a characteristic structural feature of pyridoxamine enzymes. In addition, the spatial relationships between the pyridoxal 5′-phosphate binding sites and reductase site(s) have been studied with fluorescence resonance energy-transfer techniques. The distances between site I and the enoyl reductase and β-ketoacyl reductase sites are >50 and 41–44 Å, respectively. The distance between the two reductase sites is >49 Å.

Fatty acid biosynthesis is one of the most important processes in living organisms. It is essential for the growth of cellular membranes. The fatty acid synthase enzyme catalyzes fatty acid synthesis according to

$$\text{acetyl-CoA} + n\text{malonyl-CoA} + 2n\text{NADPH} + 2n\text{H}^+ \rightarrow \text{CH}_3(\text{CH}_2\text{CH}_2)_n\text{COR} + (n+1)\text{CoA} + n\text{CO}_2 + 2n\text{NADP}^+ + (n-1)\text{H}_2\text{O}$$

where R is OH or CoA.[1] Animal fatty acid synthase has three essential substrate-binding sites: serine, a substrate "loading" site; 4′-phosphopantetheine, a substrate "carrier" site; and cysteine, a substrate "waiting" site (Nixon et al., 1970; Wakil et al., 1983; Chang & Hammes, 1988). To synthesize palmitic acid or palmityl-CoA ($n = 7$), the enzyme carries out 37 sequential reactions. The organization of fatty acid synthase varies from species to species. In most procaryotes, fatty acid synthesis is carried out by seven separable monofunctional enzymes and acyl-carrier protein [cf. Volpe and Vagelos (1973)]. However, in eucaryotes, a multienzyme complex is utilized (Wood et al., 1978; Wakil et al., 1983; Schweizer, 1986). The evolutionary aspects of fatty acid synthase have been extensively discussed (Poulose et al., 1981; Hardie & McCarthy, 1986; Witkowski et al., 1987; Chang & Hammes, 1988).

The structure of chicken liver fatty acid synthase ($M_r \sim 500\,000$) has been probed by limited proteolysis and chemical modification [cf. Wakil et al. (1983)]. The two identical polypeptides are arranged head-to-tail with two independent catalytic centers, each derived from two different polypeptide chains. A structural model for the enzyme has been constructed from small-angle neutron-scattering and electron microscope studies (Stoops et al., 1987). The polypeptides have dimensions of 160 × 146 × 73 Å, with three domains having lengths of 32, 82, and 46 Å. Limited tryptic digestion yields three protein bands on sodium dodecyl sulfate–polyacrylamide gels (Tsukamoto et al., 1983). Domain I ($M_r \sim 127\,000$), the N-terminal region of the protein, contains the acyl transferases and β-ketoacyl synthase. Domain II ($M_r \sim 107\,000$) contains the dehydratase, enoyl reductase, β-ketoacyl reductase, and the acyl-carrier protein. Domain III ($M_r \sim 33\,000$), the C-terminal region, is the thioesterase.

† This work was supported by a grant from the National Institutes of Health (GM 13292).

[1] Abbreviations: CoA, coenzyme A; NADPH, reduced nicotinamide adenine dinucleotide phosphate; HPLC, high-performance liquid chromatography; EDTA, ethylenediaminetetraacetic acid; Tris, tris(hydroxymethyl)aminomethane; TNADPH, reduced thionicotinamide adenine dinucleotide phosphate; TPCK, L-1-(tosylamino)-2-phenylethyl chloromethyl ketone.

0006-2960/89/0428-3781$01.50/0

The overall and elementary steps in the reaction mechanism, the detailed stereochemistry, the distribution of reaction intermediates on the enzyme, the distances between several specific sites, the partial sequencing of DNA complementary to mRNA, and the correlation of enzymatic activities and aggregation state have been explored [cf. Hammes (1985), Anderson and Hammes (1985), Yuan and Hammes (1985, 1986), Chang and Hammes (1986), Leanz and Hammes (1986), Yuan et al. (1988), and Kashem and Hammes (1988)]. The amino acid sequences associated with the three substrate-binding sites in chicken liver fatty acid synthase have been determined (Chang & Hammes, 1988).

In this study, to characterize the NADPH-binding sites on chicken liver fatty acid synthase, the amino acid sequences associated with pyridoxal 5′-phosphate binding sites have been determined. Pyridoxal 5′-phosphate binds to a site that causes selective inhibition of the enoyl reductase activity in the enzyme and to a site that is not associated with enzymatic activity (Cardon & Hammes, 1983). In addition, the distances between the latter pyridoxal 5′-phosphate site and the two reductase sites and the distance between the two reductase sites were estimated with fluorescence resonance energy-transfer techniques.

Materials and Methods

Chemicals. NADPH, $NADP^+$, $TNADP^+$, acetyl-CoA, malonyl-CoA, acetoacetyl-CoA, crotonyl-CoA, pyridoxal 5′-phosphate, $NaBH_4$, trifluoroacetic acid, Sephadex G-50-80, DEAE-Sephacel, D-glucose 6-phosphate, and D-glucose-6-phosphate dehydrogenase (type XXIII) were from Sigma Chemical Co. N^{ϵ}-Phosphopyridoxallysine was prepared as described by Cardon and Hammes (1983). Guanidine hydrochloride was from Pierce Chemical Co. L-1-(Tosylamino)-2-phenylethyl chloromethyl ketone treated trypsin was from Worthington Biochemical Corp. The Vydac 218-TP5405 C-18 (5 μm, 4.6 mm × 5 cm) and the Aquapore RP-300 C-8 (7 μm, 4.6 mm × 10 cm) HPLC columns were from Separation Group and Brownlee Laboratories, respectively. HPLC-grade triethylamine, phosphoric acid, and acetonitrile were from Fisher Scientific. All other chemicals were high-quality commercial grades, and solutions were prepared with deionized water. High-purity water from a MilliQ water system was used for HPLC buffers.

TNADPH was prepared from $TNADP^+$ by enzymatic reduction with glucose-6-phosphate dehydrogenase (Stein et al., 1963; Wright & Takahashi, 1977). $TNADP^+$ (5 mg) was incubated with 10 units of D-glucose-6-phosphate dehydrogenase in 0.6 mL of 0.2 M potassium phosphate (pH 7.8) containing 5 mM $MgCl_2$ and 50 mM D-glucose 6-phosphate at 25 °C in the dark. After 1.5 h, the reaction was quenched by vortexing with 2 drops of chloroform for 1 min. The reaction mixture was filtered twice and diluted by addition of 20 mL of deionized water. This solution was loaded onto a 1.5-mL DEAE-Sephacel column preequilibrated at 4 °C with 5 mM potassium phosphate (pH 7.0). The column was eluted stepwise with 55 mL of 30 mM potassium phosphate (pH 7.0) and 20 mL of 0.2 M potassium phosphate (pH 7.8). The flow rate was 0.25 mL/min, and fractions were collected every 4 min. TNADPH was eluted with 0.2 M potassium phosphate, and fractions were stored at −70 °C. The TNADPH solution had an absorbance ratio, 399:260 nm, of 0.72 [cf. Stein et al. (1963); $A_{399}/A_{260} = 0.74$].

Concentrations of acetyl-CoA, malonyl-CoA, and acetoacetyl-CoA were determined by use of an extinction coefficient of 1.5×10^4 M^{-1} cm^{-1} at 260 nm (P-L Biochemical Circular OR-10). The concentrations of NADPH, TNADPH, and crotonyl-CoA were determined by use of an extinction coefficient of 6.22×10^3 M^{-1} cm^{-1} at 340 nm (P-L Biochemical Circular OR-10), 1.17×10^4 M^{-1} cm^{-1} at 399 nm (Stein et al., 1963), and 1.9×10^4 M^{-1} cm^{-1} at 260 nm (Vernon & Hsu, 1984), respectively. The concentration of pyridoxal 5′-phosphate was determined by use of an extinction coefficient of 6.6×10^3 at 388 nm in 0.1 N NaOH (Sober, 1970) or 5.7×10^3 M^{-1} cm^{-1} at 388 nm in 0.1 M potassium phosphate (pH 7.0).

Fatty Acid Synthase. The enzyme was prepared from chicken livers and assayed as previously described (Cardon & Hammes, 1982; Cognet & Hammes, 1985; Chang & Hammes, 1986). The specific activity of the enzyme was greater than 1.6 μmol of NADPH/(min·mg) under standard assay conditions. For assay of the enoyl reductase activity of pyridoxamine phosphate modified enzyme, the observed rates were corrected for loss of NADPH in the presence of the modified enzyme. The protein concentration was determined by measurement of the absorbance at 280 nm and by use of an extinction coefficient for fatty acid synthase of 4.82×10^5 M^{-1} cm^{-1} (or 0.965 cm^2 mg^{-1}; Hsu & Yun, 1970). The 10 mM dithiothreitol and 10% glycerol (w/v) necessary for storage of the purified enzyme were removed by passage of the enzyme through a 3-mL Sephadex G-50 centrifuge column (Penefsky, 1977), preequilibrated with 0.1 M potassium phosphate and 1 mM EDTA (pH 7.0).

The coenzyme analogues $TNADP^+$ and TNADPH are substrates for various dehydrogenases and glutathione reductase (Anderson et al., 1963; Moroff et al., 1976; Wright & Takahashi, 1977; Bailey & Colman, 1987). They are also substrates of fatty acid synthase. The overall reaction was monitored spectrophotometrically by following the decrease in absorbance of TNADPH at 399 nm at 25 °C. The assay mixture contained 100 mM potassium phosphate (pH 7.0), 1 mM EDTA, 100 μM malonyl-CoA, 50 μM acetyl-CoA, 3.58×10^{-8} M enzyme, and 1.6–80 μM TNADPH. The turnover number, k_{cat}, and the Michaelis constant for TNADPH, K_m, were determined by a nonlinear least-squares fit of the data to $v/[E_0] = k_{cat}/(1.73 + K_m/[TNADPH])$, where v is the initial steady-state velocity and $[E_0]$ is the total enzyme concentration (Cox & Hammes, 1983).

Labeling of the Enzyme with Pyridoxal 5′-Phosphate. Fatty acid synthase was labeled by the method of Poulose and Kolattukudy (1980), as previously described (Cardon & Hammes, 1983). To prepare pyridoxamine phosphate enzyme for proteolytic digestion, 7.2 mL of fatty acid synthase (5.0 mg/mL) in 0.1 M potassium phosphate (pH 7.0) and 1 mM EDTA was mixed with 0.18 mL of 40 mM pyridoxal 5′-phosphate for 15 min at 25 °C. One drop of octanol was added to the reaction mixture, which was placed on ice, and 0.37 mL of 200 mM $NaBH_4$ was added to the labeled enzyme. The reduction reaction was monitored by measurement of the ultraviolet absorbance at 325 nm and the fluorescence (325 nm excitation, 395 nm emission). Unused reactants and degradation products were removed by ultrafiltration through an Amicon Centricon 10 microconcentrator. The labeled enzyme (4.0 mL) was denatured with 3.5 mL of 8 M guanidine hydrochloride for 10 min and dialyzed against 2 L of 1% acetic acid (pH 3.6) for 3 h. After a change of dialysis buffer, the labeled enzyme was dialyzed overnight. The milky solution was centrifuged at 7710*g* for 10 min, and the pellet was resuspended in 4 mL of 0.1 M Tris-HCl (pH 8.0).

Tryptic digestion was performed by addition of 40 μL of TPCK-treated trypsin (10 mg/mL) to the labeled enzyme at 37 °C. After 3 h, another 40 μL of TPCK-treated trypsin was

added and the reaction mixture incubated at 37 °C for an additional 20 h. After centrifugation of the digestion mixture for 10 min at 7710*g*, the supernatant was stored at −70 °C.

Preparation of the pyridoxamine phosphate enzyme in the presence of 5 mM NADPH was done in a similar way, except that the initial reaction mixture consisted of 2.4 mL of the 230 000 core fragment (9.1 mg/mL) of fatty acid synthase (minus the 33 000 thioesterase domain), prepared from tryptic digests (a gift of Dr. W. Liu, Cornell University) and mixed with 60 μL of 40 mM pyridoxal 5′-phosphate.

Analysis of Labeled Peptides. Peptides were first separated on a Vydac 218-TP5405 C-18 column (5 μm, 4.6 mm × 5 cm) by elution at 1.0 mL/min with a 120-min linear gradient from 98% solvent A (0.1% triethylammonium phosphate/99.9% H_2O, pH 3.6) to 40% solvent B (100% acetonitrile). The chromatography was preceded by a 10-min isocratic elution with 98% solvent A. Fractions of 0.6 mL were collected. Detection was carried out simultaneously with a Beckman Model 160 absorbance detector at 214 nm and with a Waters Model 420 fluorescence detector (excitation at 313 nm and emission at >400 nm). The fluorescent fractions were pooled and further purified on an Aquapore RP-300 C-8 column (7 μm, 4.6 mm × 10 cm) by elution at 1.0 mL/min with an 80-min linear gradient from 98% solvent C (0.1% trifluoroacetic acid/99.9% H_2O) to 40% solvent D (0.1% trifluoroacetic acid/9.9% H_2O/90% acetonitrile). Fractions of 0.6 mL were collected. If necessary, the fluorescent fractions were further purified under the same conditions for confirmation of peak purity.

The purified peptides were characterized by amino acid and sequence analyses by the Cornell University Biotechnology Program facility as previously described (Chang & Hammes, 1988). Approximately 60% of the material recovered after each cycle was used for fluorescence determinations.

Spectroscopic Measurements. A Cary 2200 spectrophotometer was used for absorbance measurements. Steady-state fluorescence measurements were done with a Hitachi-Perkin-Elmer MPF-44B fluorescence spectrophotometer equipped with corrected spectrum and polarization accessories. Steady-state polarization measurements were corrected for unequal transmission of the monochromator grating (Cerione & Hammes, 1982). Quantum yields were measured by a comparative method (Parker & Reese, 1960); the fluorescence standard was quinine sulfate in 0.1 N H_2SO_4 excited at 325 nm, which was assumed to have a quantum yield of 0.70 (Scott et al., 1970).

Fluorescence Resonance Energy-Transfer Measurements. To prepare pyridoxamine phosphate labeled enzyme for fluorescence energy-transfer measurements, 1.2 mL of 3.2 μM fatty acid synthase in 0.1 M potassium phosphate (pH 7.0) and 1 mM EDTA, in the presence or absence of 5 mM NADPH, was mixed with 0.5–1.0 mM pyridoxal 5′-phosphate for 15 min at 25 °C. Two microliters of octanol was added to the reaction mixture, which was placed on ice, and 10 mM $NaBH_4$ was added to the labeled enzyme. After 15 min, the reaction was stopped by passage through two consecutive Sephadex G-50 centrifuge columns equilibrated with 0.1 M potassium phosphate (pH 7.0) and 1 mM EDTA. The extent of labeling was determined from the absorbance at 325 nm by using an extinction coefficient for enzyme-bound pyridoxamine phosphate of 1.02×10^4 M^{-1} cm^{-1} after correction for protein absorbance (Fischer et al., 1963).

Fluorescence energy transfer was measured by titrating 0.75 μM pyridoxamine phosphate enzyme (energy donor) with 0.01–0.55 mM pyridoxal 5′-phosphate (energy acceptor) or 1.09–39.6 μM TNADPH (energy acceptor) and monitoring the decrease in emission at 395 nm (excitation at 325 nm). The wavelength dependence of pyridoxamine phosphate enzyme excitation and emission is not altered by the presence of TNADPH, so that the ratio of the fluorescence emission at 395 nm, F_{DA}/F_D, is proportional to the ratio of quantum yields, Q_{DA}/Q_D, where the subscript DA designates the presence of the energy acceptor and D its absence. Contributions of inner filter effects to the measurements were determined from the observed decrease in fluorescence of N^{ϵ}-phosphopyridoxallysine with varying concentrations of TNADPH. For the titration of pyridoxamine phosphate enzyme with pyridoxal 5′-phosphate, the emission wavelength of the modified enzyme is altered by the presence of pyridoxal 5′-phosphate (>200 μM). Therefore, the fluorescence of the modified enzyme and N^{ϵ}-phosphopyridoxallylsine at 395 nm was corrected for the fluorescence of pyridoxal 5′-phosphate (0.01–0.55 mM) at this wavelength. After this correction, F_{DA}/F_D at 395 nm is proportional to Q_{DA}/Q_D. Pyridoxamine derivatives were found to be light sensitive (Matsumoto & Hammes, 1975), so that exposure to light was minimized and 2-mm excitation slit widths were used.

The efficiency of energy transfer when the enzyme is saturated with the energy acceptor, E, is given by

$$E([EL]/n[E_0]) = 1 - Q_{DA}/Q_D \quad (1)$$

where Q_{DA} and Q_D are the quantum yields of enzyme-bound pyridoxamine phosphate in the presence and absence of TNADPH or pyridoxal 5′-phosphate, respectively, [EL] is the concentration of the energy acceptor–enzyme complex, n is the number of binding sites, and $[E_0]$ is the total enzyme concentration. The concentration of EL can be calculated from n, $[E_0]$, the dissociation constant K_d, and the total TNADPH concentration $[L_0]$ from

$$2[EL]/n[E_0] = (1 + [L_0]/n[E_0] + K_d/n[E_0]) - \{(1 + [L_0]/n[E_0] + K_d/n[E_0])^2 - 4[L_0]/n[E_0]\}^{1/2} \quad (2)$$

The distance between the energy donor and acceptor, R, was calculated from (Förster, 1959)

$$E = (R_0/R)^6/[1 + (R_0/R)^6] \quad (3)$$

with

$$R_0 = (9.79 \times 10^9)(\kappa^2 Q_D J n^{-4})^{1/6} \text{ Å} \quad (4)$$

Here n is the refractive index of the medium (1.33), J is the spectral overlap integral, Q_D is the quantum yield of the donor in the absence of the acceptor, and κ^2 is an orientation factor for dipolar coupling between donor and acceptor. The value of κ^2 was assumed to be $^2/_3$, the dynamic average.

Results

Sequence Analysis of Pyridoxamine Phosphate Enzyme. The modification of fatty acid synthase with pyridoxal 5′-phosphate has been reported (Poulose & Kolattukudy, 1980; Cardon & Hammes, 1983; Tsukamoto et al., 1983). The pyridoxal 5′-phosphate causes selective inhibition of the enoyl reductase activity in animal fatty acid synthase. However, analysis of the pyridoxal 5′-phosphate binding stoichiometry suggested that there are two pyridoxal 5′-phosphate binding sites per polypeptide, and only one of the sites is protected by NADPH (Poulose & Kolattukudy, 1980; Tsukamoto et al., 1983). Only the enoyl reductase activity of the enzyme was significantly inhibited after modification with pyridoxal 5′-phosphate.

The chromatogram of the tryptic digest of the pyridoxamine phosphate enzyme by reversed-phase HPLC on a Vydac

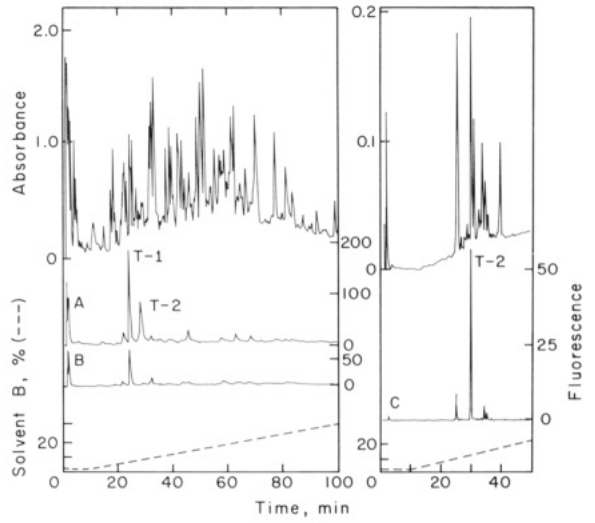

FIGURE 1: Chromatograph of trypsin digest of pyridoxamine phosphate labeled chicken liver fatty acid synthase by reversed-phase HPLC. (A) About 25% of the total labeled peptides were chromatographed on a Vydac C-18 column (4.6 mm × 5 cm) by elution at 1.0 mL/min with a 120-min linear gradient from 98% solvent A to 40% solvent B as described under Materials and Methods. The major fluorescent peaks are labeled T-1 and T-2 (fluorescence is in arbitrary units). (B) About 25% of the total labeled peptides, labeled in the presence of 5 mM NADPH, were chromatographed as described in (A). (C) The fluorescent peptides T-2 from about 25% of the total labeled peptides were chromatographed on an Aquapore RP-300 C-8 column (4.6 mm × 10 cm) by elution at 1.0 mL/min with an 80-min linear gradient from 98% solvent C to 40% solvent E as described under Materials and Methods.

Table I: Amino Acid Sequences of Pyridoxamine 5′-Phosphate Peptides from Chicken Liver Fatty Acid Synthase[a]

peptide	sequence
T-1	DGVFAKEVR
T-2	VFATVGSAEKR

[a] The lysines modified by pyridoxamine 5′-phosphate are underlined.

218-TP5405 C-18 analytical column with solvent systems A and B is shown in Figure 1. Two major fluorescence peaks (T-1 and T-2) were found (Figure 1A). However, only peak T-2 was decreased substantially when the enzyme modification was carried out in the presence of 5 mM NADPH (Figure 1B). Therefore, peptide T-2 is associated with the enoyl reductase site. The peptides were further purified on an Aquapore RP-300 C-8 column with solvent systems C and D. A typical chromatogram for the purification of T-2 is shown in Figure 1C. The peptide T-1 was purified in a similar manner.

The amino acid sequences of the pyridoxamine phosphate peptides (T-1 and T-2) are given in Table I. The amino acid compositions of the peptides were in good agreement with the sequences, except that the amino acid analysis did not reveal the lysine modified with pyridoxal 5′-phosphate. A large decrease in yield occurred after cycle number 9 for peptide T-2; however, the identification of the next two residues was still possible. A large drop in yield at cycle 6 for peptide T-1 occurred, and the residue in cycle 6 could not be identified. However, the identification of residues 7–9 was still possible. Monitoring of the fluorescence during sequencing suggests that the amino acids at cycle 6 of peptide T-1 and at cycle 10 of peptide T-2 are modified with pyridoxamine 5′-phosphate.

Fluorescence Energy Transfer. Although 2 molecules of pyridoxal 5′-phosphate per enzyme molecule are involved in actively blocking the enoyl reductase site (Poulose & Kolattukudy, 1980) and another 2 active molecules of pyridoxal 5′-phosphate per enzyme molecule bind specifically to domain

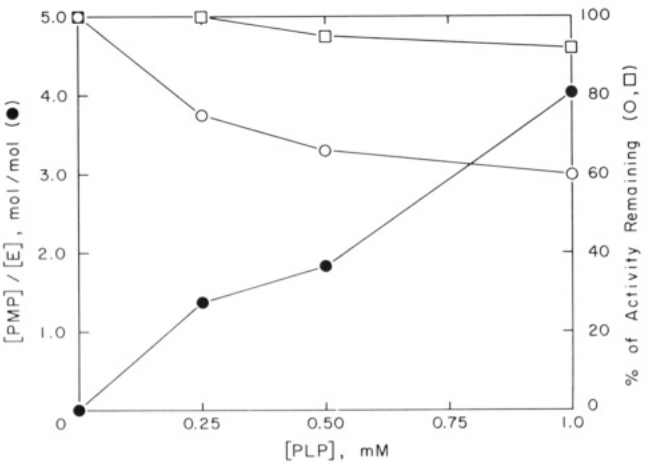

FIGURE 2: Plot of the moles of pyridoxamine phosphate bound per mole of enzyme, [PMP]/[E] (●), or the overall (○) and enoyl reductase (□) activity vs the concentration of pyridoxal 5′-phosphate, [PLP]. In this experiment, 0.3 mL of 3.2 μM enzyme in 0.1 M potassium phosphate (pH 7.0), 1 mM EDTA, and 5 mM NADPH was mixed with 0.25–1.0 mM pyridoxal 5′-phosphate for 15 min at 23 °C. The pyridoxamine phosphate modified enzyme was prepared and assayed as described under Material and Methods.

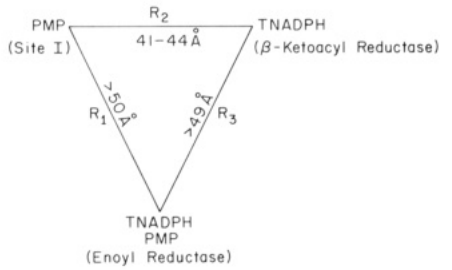

FIGURE 3: Schematic representation of the sites involved in energy-transfer measurements. The sites and distances between sites are discussed in the text.

I of the enzyme (site I; Tsukamoto et al., 1983), additional amounts of pyridoxal 5′-phosphate bind to the enzyme, depending on the conditions used. If NADPH is not present when the enzyme is modified with 0.5–1.0 mM pyridoxal 5′-phosphate/10 mM $NaBH_4$, 3.2–6.8 pyridoxamine phosphate molecules are bound per enzyme molecule, and 40–95% of the enoyl reductase activity is inhibited. If 5 mM NADPH is present when the enzyme is modified with 0.25–1.0 mM pyridoxal 5′-phosphate, 1.4–4.0 pyridoxamine phosphate molecules are bound per enzyme molecule, and the enoyl reductase is almost fully active (92–100%) (Figure 2). The nonspecific pyridoxamine phosphate binding site (site I), the β-ketoacyl reductase site, and the enoyl reductase site are shown schematically in Figure 3; the distances between these sites, R_i, are defined by this diagram.

The corrected fluorescence emission spectrum of the pyridoxamine phosphate enzyme has excellent overlap with the absorbance spectrum of pyridoxal 5′-phosphate (Figure 4). A spectral overlap integral of 9.32×10^{-15} M^{-1} cm^3 was calculated for the energy donor–acceptor pair of pyridoxamine and pyridoxal 5′-phosphate. The quantum yield of enzyme-bound pyridoxamine phosphate is 0.185, and the polarization is 0.16 (independent of binding stoichiometry). The calculated value of R_0 is 26.2 Å (eq 4). The energy-transfer efficiency between pyridoxal 5′-phosphate bound at the enoyl reductase site and pyridoxamine bound at site I was measured by titrating the pyridoxamine phosphate enzyme (energy donor) with pyridoxal 5′-phosphate (energy acceptor) and measuring the decrease in pyridoxamine phosphate fluorescence; Q_{DA}/Q_D (eq 1 and

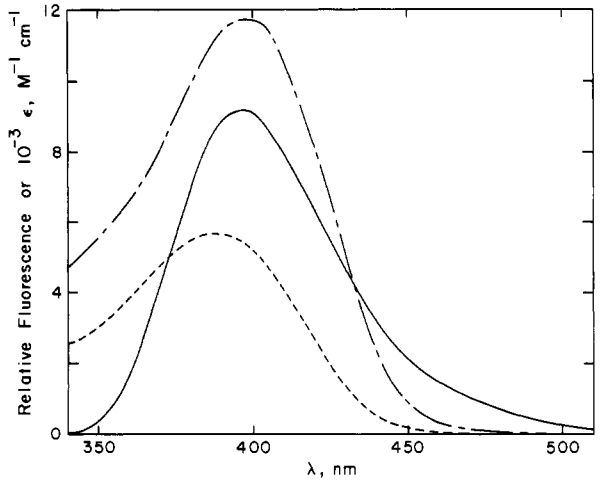

FIGURE 4: Spectral overlap of the corrected fluorescence emission for pyridoxamine phosphate–fatty acid synthase (—) with the extinction coefficient (ε) of TNADPH (– – –) and pyridoxal 5′-phosphate (- - -). The fluorescence excitation for the pyridoxamine phosphate modified fatty acid synthase was 325 nm. All spectra were taken in 0.1 M potassium phosphate (pH 7.0) and 1 mM EDTA at 23 °C.

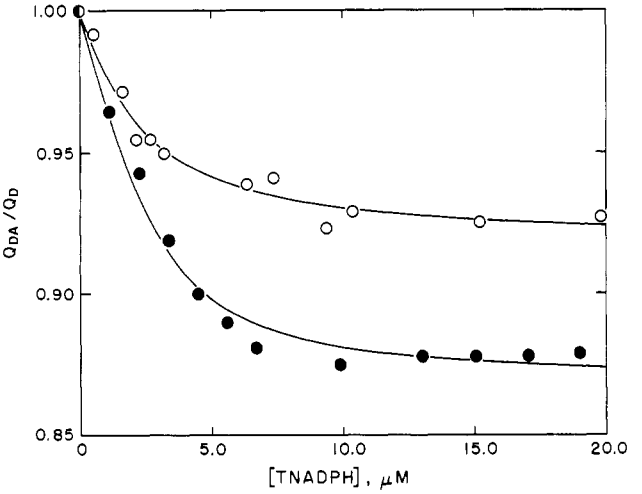

FIGURE 5: Plots of the fluorescence quenching of 0.75 μM pyridoxamine phosphate–fatty acid synthase vs the total concentration of TNADPH. Here Q_{DA} and Q_D are the quantum yields in the presence and absence of TNADPH, respectively (325-nm excitation, 465-nm emission). Titrations were performed in 0.1 M potassium phosphate (pH 7.0) and 1 mM EDTA at 23 °C. (●) The pyridoxamine phosphate enzyme was prepared in the absence of 5 mM NADPH as described under Materials and Methods, and the enoyl reductase of the modified enzyme was 98% active. Approximately 2 mol of pyridoxamine phosphate are bound per mole of enzyme. The curve is a nonlinear least-squares fit of the data to eq 1 with $n = 4.0$, $K_d = 0.79 \pm 0.18$ μM, and $E = 0.132 \pm 0.004$. (○) The pyridoxamine phosphate enzyme was prepared in the absence of NADPH as described under Materials and Methods, and the enoyl reductase of the modified enzyme was <4% active. Approximately 7 mol of pyridoxamine phosphate are bound per mole of enzyme. The curve is a nonlinear least-squares fit of the data to eq 1 with $n = 2.0$, $K_d = 1.6 \pm 0.4$ μM, and $E = 0.083 \pm 0.004$.

2). The pyridoxamine enzyme was prepared in the presence of 5 mM NADPH with 2 mol of pyridoxamine phosphate/mol of enzyme. The enoyl reductase activity was 95% that of the control enzyme. No significant energy transfer from pyridoxamine to pyridoxal 5′-phosphate was observed with concentrations of pyridoxal 5′-phosphate up to 0.55 mM. When $NADP^+$ (5 mM) was added at the end of the titration, the fluorescence intensity was not changed. If an upper detection limit of 2% energy-transfer efficiency is assumed, the distance between the enoyl reductase site and site I, R_1, is >50 Å (eq 3).

The steady-state kinetic constants for TNADPH are $K_m = 6.0 \pm 1.3$ μM and $k_{cat} = 5.5 \pm 0.3$ s^{-1}; the corresponding values for NADPH are 2.9 ± 0.4 μM and 23.0 ± 0.7 s^{-1} (Cox & Hammes, 1983). The corrected fluorescence emission spectrum of the pyridoxamine phosphate enzyme has excellent overlap with the absorbance spectrum of TNADPH (Figure 4). The spectral overlap integral is 2.14×10^{-14} M^{-1} cm^3 for the enzyme-bound pyridoxamine phosphate and enzyme-bound TNADPH. The value of R_0 calculated from eq 4 is 30.1 Å. Two different pyridoxamine phosphate enzyme species were prepared: (1) only site I of the enzyme was modified with pyridoxamine phosphate; (2) both site I and the enoyl reductase of the enzyme were modified with pyridoxamine phosphate. The energy-transfer efficiency between enzyme-bound TNADPH and the pyridoxamine enzyme species was measured by titrating the pyridoxamine phosphate enzyme (energy donor) with TNADPH (energy acceptor) and measuring the decrease in pyridoxamine phosphate fluorescence (eq 1 and 2).

The lower curve in Figure 5 shows the titration of enzyme with ~2 mol of pyridoxamine phosphate/mol of enzyme plotted as the quenching ratio versus the total concentration of TNADPH. The enzyme was modified in the presence of 5 mM NADPH, and the enoyl reductase of the modified enzyme was 98% active relative to the native enzyme. The data were fit to eq 1 with $n = 4.0$; a nonlinear least-squares fit of the data gave $K_d = 0.79 \pm 0.18$ μM and $E = 0.132 \pm 0.004$. For the titration curve, two acceptors (TNADPH bound both at the enoyl reductase and the β-ketoacyl reductase sites) and one donor (one pyridoxamine phosphate located on site I) are present. (This assumes the two catalytic domains of the enzyme are too far apart for energy transfer to occur between them.) The energy-transfer efficiency for this case is given by

$$E = [(R_0/R_1)^6 + (R_0/R_2)^6]/[1 + (R_0/R_1)^6 + (R_0/R_2)^6] \quad (5)$$

where R_0 is the distance for 50% energy transfer for an isolated donor–acceptor pair and R_1 and R_2 are the distances from site I to the TNADPH binding sites of enoyl reductase and β-ketoacyl reductase, respectively. The calculated value of R_2 is 44 Å with $R_1 = 50$ Å. If the distance $R_1 = \infty$, $R_2 = 41$ Å. Therefore, the distance between site I and the β-ketoacyl reductase site of the same catalytic domain, R_2, is 41–44 Å.

The upper curve in Figure 5 shows the titration of enzyme with ~7 mol of pyridoxamine phosphate/mol of enzyme plotted as the quenching ratio versus the total concentration of TNADPH. The enzyme was modified in the absence of NADPH; the enoyl reductase of the modified enzyme is <4% active. A binding stoichiometry of ~7 mol/mol was required to inactivate enoyl reductase completely. The data were fit to eq 1 with $n = 2.0$; a nonlinear least-squares fit of the data gave $K_d = 1.6 \pm 0.4$ μM and $E = 0.083 \pm 0.004$. For this case, one acceptor, TNADPH bound only at the β-ketoacyl reductase site, and two donors, pyridoxamine phosphate located at both site I and the enoyl reductase site, are present. Unfortunately, pyridoxamine phosphate also is bound at some additional sites on the enzyme, so that distances calculated by assuming only specific binding are lower bounds. For this case

$$E = (1/3.5)\{(R_0/R_2)^6/[1 + (R_0/R_2)^6] + (R_0/R_3)^6/[1 + (R_0/R_3)^6] + \text{nonspecific terms}\} \quad (6)$$

If the pyridoxamine phosphate that is nonspecifically bound is far away from the enzyme-bound TNADPH ($\gg R_0$), then the contribution of "nonspecific terms" in eq 6 is zero. If R_2

Table II: Comparison of the Primary Structure of the Enoyl Reductase Active Site from Chicken Liver Fatty Acid Synthase with That of Other Fatty Acid Synthases, Dehydrogenases, and Reductases[a]

	↓
Chicken	V F A T V G S A E K R
Goose[b]	V F T T V G S A E K R
Yeast (β subunit residues 767-777)[c]	F G S G F G S A D D T
Horse alcohol dehydrogenase[d]	F S T G Y G S A V K V
Human glyceraldehyde-3-P-dehydrogenase[d]	V F T T M E K A G A H
Yeast glyceraldehyde-3-P-dehydrogenase[d]	V F K E L D T A Q K H
Spinach ferredoxin-NADP$^+$ reductase[e]	(R,K)S V S L C V K R
Bovine NADPH-adrenoferredoxin reductase[f]	R I K E A A R P R K R
H. saimiri dihydrofolate reductase[g]	D K Q N L V I M G K K
Chicken dihydrofolate reductase[h]	G K Q N L V I M G K K
L. casei dihydrofolate reductase[i]	K I M V V G R R

[a] The sequences are aligned via the reactive lysine of chicken liver enoyl reductase (arrow). Identical amino acids are indicated by the boxes. [b] Poulose and Kolattukudy (1983). [c] Chirala et al. (1987). [d] Branden and Eklund (1980). [e] Cidaria et al. (1985). [f] Hamamoto et al. (1988). [g] Trimble et al. (1988). [h] Kumar et al. (1980). [i] Volz et al. (1982).

is set equal to 42.5 Å, then $R_3 > 49$ Å. The maximum value of the nonspecific terms is 1.5, so that a meaningful upper bound for R_3 cannot be calculated. However, the nonspecifically bound pyridoxamine phosphate is unlikely to be close to the enzyme-bound TNADPH since the β-ketoacyl reductase activity is unaltered in the modified enzyme. Nevertheless, the dissociation constants for both TNADPH and NADPH binding to the modified enzyme are slightly increased relative to the native enzyme (Cardon & Hammes, 1983).

The bounds obtained for the three distances determined by these energy-transfer measurements are included in Figure 3.

Discussion

Two types of NADPH binding sites are present on chicken liver fatty acid synthase [cf. Poulose et al. (1980) and Cardon and Hammes (1983)], one associated with β-ketoacyl reductase, the other with enoyl reductase. A reactive lysine associated with the enoyl reductase activity has been labeled with pyridoxal 5′-phosphate/$NaBH_4$ (Poulose et al., 1983; Cardon & Hammes, 1983; Tsukamoto et al., 1983). In this study, the amino acid sequence associated with the enoyl reductase site was determined for the pyridoxamine phosphate enzyme. In Table II the sequence of the chicken peptide is compared with that of goose (Poulose & Kolattukudy, 1983) and yeast (Chirala et al., 1987) from the same enzyme. Horse alcohol dehydrogenase and human and yeast glyceraldehyde-3-phosphate dehydrogenase (Branden & Eklund, 1980) sequences are included in Table II. The sequence similarities between chicken and goose are extensive. Of the 11 amino acids near the active lysine site for the chicken and goose, 10 are identical and 1 differs by a single point mutation; for the chicken and yeast, 3 are identical; 4 identical amino acids exist between chicken and horse alcohol dehydrogenase, human glyceraldehyde-3-phosphate dehydrogenase, and yeast glyceraldehyde-3-phosphate dehydrogenase. The sequence Gly-Ser-Ala in the immediate vicinity of the active lysine group is common to the chicken, goose, and yeast fatty acid synthase and horse alcohol dehydrogenase. The change from Lys to Asp in yeast fatty acid synthase explains why pyridoxal 5′-phosphate inhibits only the animal enoyl reductase (Poulose & Kolattukudy, 1980; Cardon & Hammes, 1983; Tsukamoto et al., 1983; Chirala et al., 1987). The sequence Ser-X-X-Lys is a characteristic structural feature of pyridoxal phosphate enzymes (Tanase et al., 1979), and chicken and goose fatty acid synthases and horse alcohol dehydrogenase have this sequence. In Table II, the sequences for several reductases also are included. The sequence Lys (or Arg)-Arg (or Lys) in the active site is conserved in both enoyl reductase and other reductases. This observation suggests that the positive charges of the lysine and argine residues are involved in the binding of NADP(H) to the enzymes (Cidaria et al., 1985).

Although the functional role of peptide T-1 (site I) is not known, the amino acid sequence has a slight homology with peptide T-2, namely, the sequence Val-Phe-Ala. Peptide T-1 has been located in domain I of the proteolytic map of fatty acid synthase (Tsukamoto et al., 1983).

Several criteria are necessary for reliable interpretation of fluorescence resonance energy-transfer measurements on proteins [cf. Matsumoto and Hammes (1975) and Yuan and Hammes (1986)]: (1) the fluorescence probes must be bound at specific sites; (2) fluorescence quenching by the energy acceptor must be due only to energy transfer; and (3) the uncertainty associated with the assumption that $\kappa^2 = {}^2/_3$ must be considered (Dale et al., 1979).

The specificity of the pyridoxamine phosphate binding sites is the primary difficulty associated with the measurements reported here. The specificity of binding to site I is quite good, and although the pyridoxal phosphate binding may not be entirely specific, it is immaterial since no energy transfer is observed. Consequently, only a lower bound for R_1 can be calculated. Only a lower bound can be given for the distance between the β-ketoacyl reductase and enoyl reductase binding sites, R_3, because of the nonspecificity of pyridoxamine phosphate binding. On the other hand, the binding of TNADPH to the enzyme is quite specific since it is a substrate with a relatively low dissociation constant. Two other assumptions are implicit in the interpretation presented: (1) energy transfer between the two active-site domains of fatty acid synthase is negligible; and (2) pyridoxamine phosphate and TNADPH bind at approximately the same position in the enoyl reductase site. Although both of these assumptions are reasonable, a direct assessment of their validity is not possible.

All trivial forms of fluorescence quenching have been corrected for, and the wavelength dependence of the enzyme-bound pyridoxamine phosphate fluorescence is not altered by the binding of TNADPH to the enzyme, consistent with only energy transfer being responsible for the fluorescence quenching. Although pyridoxal 5′-phosphate appears to alter slightly the pyridoxamine phosphate fluorescence, this can be attributed to the fluorescence of pyridoxal 5′-phosphate and has been corrected for. Since the steady-state fluorescence polarization of enzyme-bound pyridoxamine phosphate is only 0.16, which is considerably less than the limiting polarization of 0.41 (Churchich, 1965), the fluorescent probe has significant rotational mobility. Therefore, the assumption that $\kappa^2 = {}^2/_3$ is unlikely to cause an uncertainty greater than ±10% in the calculated distances [cf. Dale et al. (1979) and Snyder and Hammes (1984, 1985)].

The distances determined here are consistent with the results of previous studies. The distance between the two reductases has been estimated as >15 Å with electron paramagnetic resonance (Chang & Hammes, 1986). In addition, the distances from the 4′-phosphopantetheine to the enoyl reductase and the β-ketoacyl reductase sites on the same polypeptide have been estimated as 38 Å and the distances from the 4′-phosphopantetheine to the thioesterase active site as 48 Å (Yuan & Hammes, 1986). Finally, 1,3-dibromo-2-propanone has

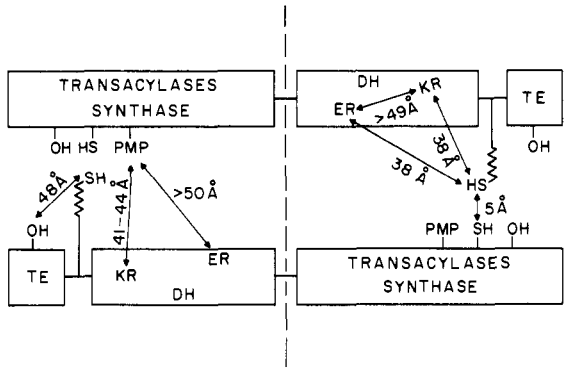

FIGURE 6: Structural map of chicken liver fatty acid synthase with the following abbreviations: wavy line SH, 4′-phosphopantetheine; TE, thioesterase; ER, enoyl reductase; DH, dehydratase; KR, β-ketoacyl reductase; PMP, pyridoxamine phosphate; adjacent OH and SH groups in domain I, the substrate loading and waiting sites, respectively; OH in the thioesterase, the catalytic site. The arrangement of the two identical polypeptides is from limited proteolysis and chemical modification studies [cf. Wakil et al. (1983)]. The distances between the two reductases and from site I to the two reductases are from this study. The other distances are from previous fluorescence energy-transfer studies (Yuan & Hammes, 1986) and 1,3-dibromo-2-propanone modification of the enzyme (Wakil et al., 1983).

been used to cross-link the cysteine (waiting site) on domain I of one polypeptide chain to the 4′-phosphopantetheine (carrier site) on a different polypeptide chain, demonstrating that these two sites are within 5 Å (Wakil et al., 1983). The distance between the two reductase sites is surprisingly large (>49 Å) in view of the fact that the phosphopantetheine arm is 24 Å long.

A summary of the spatial relationships between sites on fatty acid synthase is shown in Figure 6. This provides a working model that can be subjected to further experimental testing.

References

Anderson, B. M., Anderson, C. D., Lee, J. K., & Stein, A. M. (1963) *Biochemistry 2*, 1017–1022.

Anderson, V., & Hammes, G. G. (1985) *Biochemistry 24*, 2147–2154.

Bailey, J. M., & Colman, R. F. (1987) *Biochemistry 26*, 4893–4900.

Branden, C., & Eklund, H. (1980) *Dehydrogenases Requiring Nicotinamide Coenzyme* (Jeffrey, J., Ed.) pp 40–84, Birkhauser Verlag, Boston.

Cardon, J. W., & Hammes, G. G. (1982) *Biochemistry 21*, 2863–2870.

Cardon, J. W., & Hammes, G. G. (1983) *J. Biol. Chem. 258*, 4802–4807.

Cerione, R. A., & Hammes, G. G. (1982) *Biochemistry 21*, 745–752.

Chang, S.-I., & Hammes, G. G. (1986) *Biochemistry 25*, 4661–4668.

Chang, S.-I., & Hammes, G. G. (1988) *Biochemistry 27*, 4753–4760.

Chirala, S. S., Kuziora, M. A., Spector, D. M., & Wakil, S. J. (1987) *J. Biol. Chem. 262*, 4231–4240.

Churchich, J. E. (1965) *Biochim. Biophys. Acta 102*, 280–288.

Cidaria, D., Biondi, P. A., Zaneiti, G., & Ronchi, S. (1985) *Eur. J. Biochem. 146*, 295–299.

Cognet, J. A. H., & Hammes, G. G. (1985) *Biochemistry 24*, 290–297.

Cox, B. G., & Hammes, G. G. (1983) *Proc. Natl. Acad. Sci. U.S.A. 80*, 4233–4237.

Dale, R. E., Eisinger, J., & Blumberg, W. E. (1979) *Biophys. J. 26*, 161–194.

Fischer, E. H., Forrey, A. W., Hedrick, J. L., Hughes, R. C., Kent, A. B., & Krebs, E. G. (1963) *Chemical and Biological Aspects of Pyridoxal Catalysis* (Snell, E. E., Fasella, P. M., Braunstein, A., & Fanelli, A. R., Eds.) pp 543–562, Macmillan, New York.

Förster, T. (1959) *Discuss. Faraday Soc. 27*, 7–17.

Hamamoto, I., Kurokohchi, K., Tanaka, S., & Ichikawa, Y. (1988) *Biochim. Biophys. Acta 953*, 207–213.

Hammes, G. G. (1985) *Curr. Top. Cell. Regul. 26*, 311–324.

Hardie, D. G., & McCarthy, A. D. (1986) *Multidomain Proteins—Structure and Evolution* (Hardie, D. G., & Coggins, J. R., Eds.) pp 229–258, Elsevier, New York.

Hsu, R. Y., & Yun, S.-L. (1970) *Biochemistry 9*, 239–245.

Kashem, M. A., & Hammes, G. G. (1988) *Biochim. Biophys. Acta 956*, 39–48.

Kumar, A. A., Blankenship, D. T., Kaufman, B. T., & Freisheim, J. H. (1980) *Biochemistry 19*, 667–678.

Leanz, G. F., & Hammes, G. G. (1986) *Biochemistry 25*, 5617–5624.

Matsumoto, S., & Hammes, G. G. (1975) *Biochemistry 14*, 214–224.

Moroff, G., Ochs, R. S., & Brandt, K. G. (1976) *Arch. Biochem. Biophys. 173*, 42–49.

Nixon, J. E., Phillips, G. T., Abramovitz, A. S., & Porter, J. W. (1970) *Arch. Biochem. Biophys. 138*, 357–371.

Parker, C. A., & Rees, W. T. (1960) *Analyst (London) 85*, 587–600.

Penefsky, H. S. (1977) *J. Biol. Chem. 252*, 2891–2899.

Poulose, A. J., & Kolattukudy, P. E. (1980) *Arch. Biochem. Biophys. 201*, 313–321.

Poulose, A. J., & Kolattukudy, P. E. (1983) *Arch. Biochem. Biophys. 220*, 652–656.

Poulose, A. J., Rogers, L., & Kolattukudy, P. E. (1981) *Biochem. Biophys. Res. Commun. 103*, 377–382.

Schweizer, M. (1986) *Multidomain Proteins—Structure and Evolution* (Hardie, D. G., & Coggins, J. R., Eds.) pp 195–227, Elsevier, New York.

Scott, T. G., Spencer, R. D., Leonard, N. J., & Weber, G. (1970) *J. Am. Chem. Soc. 92*, 687–695.

Snyder, B., & Hammes, G. G. (1984) *Biochemistry 23*, 5787–5795.

Snyder, B., & Hammes, G. G. (1985) *Biochemistry 24*, 2324–2331.

Sober, H. A. (1970) *Handbook of Biochemistry*, 2nd ed., The Chemical Rubber Co., Cleveland, OH.

Stein, A. M., Lee, J. K., Anderson, C. D., & Anderson, B. M. (1963) *Biochemistry 2*, 1015–1017.

Stoops, J. K., Wakil, S. J., Uberbacher, E. C., & Bunick, G. J. (1987) *J. Biol. Chem. 262*, 10246–10251.

Tanase, S., Kojima, H., & Morino, Y. (1979) *Biochemistry 18*, 3002–3007.

Trimble, J. J., Murthy, S. C. S., Bakker, A., Grassmann, R., & Desrosiers, R. C. (1988) *Science 239*, 1145–1147.

Tsukamoto, Y., Wong, H., Mattick, J. S., & Wakil, S. J. (1983) *J. Biol. Chem. 258*, 15312–15322.

Vernon, C. N., & Hsu, R. Y. (1984) *Biochim. Biophys. Acta 788*, 124–131.

Volpe, J. J., & Vagelos, P. R. (1973) *Annu. Rev. Biochem. 42*, 21–60.

Volz, K. W., Mattew, D. A., Alden, R. A., Freer, S. T., Hansch, C., Kaufman, B. T., & Kraut, J. (1982) *J. Biol. Chem. 257*, 2528–2536.

Wakil, S. J., Stoops, J. K., & Joshi, V. C. (1983) *Annu. Rev. Biochem. 52*, 537–579.

Witkowski, A., Naggert, J., Mikkelsen, J., & Smith, S. (1987) *Eur. J. Biochem. 165*, 601-606.
Wood, W. I., Peterson, D. O., & Bloch, K. (1978) *J. Biol. Chem. 253*, 2650-2656.
Wright, K., & Takahashi, M. (1977) *Biochemistry 16*, 1548-1554.
Yuan, Z., & Hammes, G. G. (1985) *J. Biol. Chem. 260*, 13532-13538.
Yuan, Z., & Hammes, G. G. (1986) *J. Biol. Chem. 261*, 13643-13651.
Yuan, Z., Liu, W., & Hammes, G. G. (1988) *Proc. Natl. Acad. Sci. U.S.A. 85*, 6328-6331.

A Scanning Calorimetric Study of the Thermal Denaturation of the Lysozyme of Phage T4 and the Arg 96 → His Mutant Form Thereof†

Shinichi Kitamura‡ and Julian M. Sturtevant*
Departments of Chemistry and of Molecular Biophysics and Biochemistry, Yale University, New Haven, Connecticut 06520
Received September 29, 1988; Revised Manuscript Received January 13, 1989

ABSTRACT: High-sensitivity scanning calorimetry has been employed to study the reversible thermal unfolding of the lysozyme of T4 bacteriophage and of its mutant form Arg 96 → His in the pH range 1.80–2.84. The values for $t_{1/2}$, the temperature of half-denaturation, in degrees Celsius and for the enthalpy of unfolding in kilocalories per mole are given by (standard deviations in parentheses)

wild type

$$t_{1/2} = 9.63 + 14.41\text{pH} \ (\pm 0.58)$$

$$\Delta H_{cal} = 5.97 + 2.33t \ (\pm 4.20)$$

mutant form

$$t_{1/2} = -19.84 + 21.31\text{pH} \ (\pm 0.51)$$

$$\Delta H_{cal} = -8.58 + 2.66t \ (\pm 4.48)$$

At any temperature within the range −20 to 60 °C, the free energy of unfolding of the mutant form is more negative than that of the wild type by 3–5 kcal mol^{-1}, indicating an apparent destabilization resulting from the arginine to histidine replacement. The ratio of the van't Hoff enthalpy to the calorimetric enthalpy deviates from unity, the value expected for a simple two-state process, by ±0.2 depending on the pH. It thus appears that the nature of the unfolding of T4 lysozyme varies with pH in unknown manner. This complication does not invalidate the values reported here for the temperature of half-completion of unfolding, the calorimetric enthalpy, the heat capacity change, or the free energy of unfolding.

The lysozyme of bacteriophage T4 is a small globular protein with a single polypeptide chain containing 164 amino acid residues and having a molecular weight of 18 700. The structure of this protein has been determined to a resolution of 1.7 Å, and the structures of several mutant forms have also been obtained (Grutter et al., 1979, 1983; Alber et al., 1987; Alber & Matthews, 1987; Matsumura et al., 1988). The thermal denaturation of T4 lysozymes has been carefully studied by Schellman and his colleagues (Hawkes et al., 1984; Elwell & Schellman, 1975, 1977, 1979; Schellman et al., 1981) using circular dichroism (CD) and fluorescence spectrophotometry to follow the course of the unfolding. It has been demonstrated that the thermal unfolding of T4 lysozyme and at least some of its mutants is completely reversible at low pH.

It is clear from this earlier work that the thermal unfolding of T4 lysozyme and its mutant forms is a very nearly ideal case for detailed study by means of high-sensitivity differential scanning calorimetry (DSC). Our colleagues at the University of Oregon have kindly agreed to supply us with the large amounts of proteins needed for such studies. This paper reports results obtained for the wild-type (WT) enzyme and the temperature-sensitive mutant Arg 96 → His (R96H).

The calorimetric method for studying thermal denaturation has a major disadvantage as compared with optical methods, namely, that concentrations higher by an order of magnitude or more are required, which in some cases may lead to increased difficulties due to aggregation, particularly of denatured proteins. On the other hand, a major advantage of the calorimetric method is that it gives values both for the apparent, or van't Hoff, enthalpy, the quantity derived from optical experiments, and for the true, or calorimetric, enthalpy and thus affords a direct check on whether the process under study shows simple two-state behavior, indicated by equality of these two enthalpies. It may be mentioned that it is quite possible for a process to adhere accurately to the van't Hoff equation, and thus appear to be two state, when in fact these two enthalpies differ significantly [cf. Sturtevant (1987)]. It is evident that the calorimetric method cannot distinguish

† This research was aided by grants from the National Institutes of Health (GM-04725) and the National Science Foundation (DMB8421173).
‡ Present address: Department of Agricultural Chemistry, Kyoto Prefectural University, Shimogamo, Kyoto 606, Japan.

0006-2960/89/0428-3788$01.50/0